UCRL-JC-130384
PREPRINT

Optics Elements for Modeling Electrostatic Lenses and Accelerator Components II. Acceleration Columns

G.H. Gillespie
T.A. Brown

This paper was prepared for submittal to the
Fifth International Conference on Charged Particle Optics
Delft, The Netherlands
April 14-17, 1998

May 1998

GHGA-98-559-TM

OPTICS ELEMENTS FOR MODELING ELECTROSTATIC LENSES AND ACCELERATOR COMPONENTS: II. ACCELERATION COLUMNS

George H. Gillespie

G. H. Gillespie Associates, Inc.
P. O. Box 2961
Del Mar, California 92014, U.S.A.

and

Thomas A. Brown

Center for Accelerator Mass Spectrometry
LLNL, P. O. Box 808
Livermore, California 94551, U.S.A.

10 April 1998

This paper has been submitted for publication in the proceedings of the Fifth International Conference on Charged Particle Optics (Delft, The Netherlands, 14-17 April 1998)

Optics Elements for Modeling Electrostatic Lenses and Accelerator Components
II. Acceleration Columns

George H. Gillespie

G. H. Gillespie Associates, Inc., P. O. Box 2961, Del Mar, California, 92014, U.S.A.

Thomas. A. Brown

Center for Accelerator Mass Spectrometry, LLNL, P.O. Box 808, Livermore, CA 94551, U.S.A.

Abstract

A set of optical models for a variety of electrostatic lenses and accelerator columns has been developed for the computer code TRACE 3-D. TRACE 3-D is an envelope (matrix) code including space charge that is often used to model bunched beams in magnetic transport systems and radiofrequency (RF) accelerators when the effects of beam current may be important. Several new matrix models have been developed that allow the code to be used for modeling beam lines and accelerators with electrostatic components. The new models include a number of options for: (1) einzel lenses, (2) accelerator columns, (3) electrostatic deflectors (prisms), and (4) an electrostatic quadrupole. A prescription for setting up the initial beam appropriate to modeling 2-D (continuous) beams has also been developed. The new models for (2) are described in this paper, selected comparisons with other calculations are presented, and a beamline application is summarized.

Key Words: Computer Codes, Particle Optics, Accelerator Design, Electrostatic Accelerator

Name and address for proofs:	George H. Gillespie G. H. Gillespie Associates, Inc. P. O. Box 2961, Del Mar, California, 92014, U.S.A.
Phone, Fax, email:	619-677-0076 / 619-677-0079 / ghga@ghga.com

1. INTRODUCTION

TRACE 3-D [1] is a first-order code that uses the transfer matrix (R-matrix) formalism to compute changes to the beam matrix (σ-matrix) [1,2]. Each optical element is divided into a series of small (longitudinal) segments and the calculation then steps through the beamline one segment at time. The effective R-matrix may be modified in each segment to include, for example, space charge impulses or fringe field effects. R-matrix models have been developed for a number of electrostatic elements and these TRACE 3-D capabilities have been used to (a) incorporate changes in the beam energy as a function of position in the electrostatic elements, (b) include fringe field models of those elements, and (c) develop a space charge model to describe continuous (dc) beams for all elements. TRACE 3-D has a number of beam matching and fitting capabilities that make it especially useful as a beamline design and optimization code. The addition of the electrostatic elements extends the applicability of the code to a variety of new problems.

Two different electrostatic acceleration columns, a two-aperture column and a two-tube (or two-cylinder) column, have been modeled. The geometries and key parameters are illustrated in Figure 1. Both of the acceleration columns have cylindrical symmetry about the z axis, indicated by the dashed line in Figure 1. More complex geometries can be simulated in TRACE 3-D using two or more of the column elements.

2. OPTICS MODELING

The optics of particles near the axis of cylindrically symmetric electrostatic elements is determined by the axial potential distribution $V(z)$. The near axis electric fields, which satisfy Maxwell's equation $\nabla \bullet \boldsymbol{E} = 0$ for any $V(z)$, are given by:

$$E_x(x,y,z) = + [(1/2)\,(\partial^2 V(z)/\partial^2 z)]x \quad , \tag{1}$$

$$E_y(x,y,z) = + [(1/2)\,(\partial^2 V(z)/\partial^2 z)]y \quad , \tag{2}$$

and

$$E_z(x,y,z) = - (\partial V(z)/\partial z) \quad . \tag{3}$$

The first-order transfer matrix, or R-matrix, is used to describe the optics of particles in the paraxial approximation. For modeling the full six dimensional phase space, the required R-matrix is 6×6.

2.1 R-Matrix Elements

The elements of the 6×6 R-matrix may be computed directly from the electric fields using standard techniques; our method is to similar the approach of reference [3]. The region over which the fields (1)-(3) act is divided into small steps of length Δz and three R-matrices are computed for each step. The first R-matrix is an acceleration matrix, and together with an increase in the beam energy, computes the effects of a uniform electric field acting over a distance of Δz. The second R-matrix is a lens matrix, and computes the focusing effect of the field applied as an impulse which results in an effective thin lens. The third R-matrix is a space-charge impulse matrix, used at each step to model the effective first-order space-charge forces, which become important for high beam currents. The approach described here was also used in a previous work [4] to develop TRACE 3-D optics models for three different einzel lens geometries.

The non-trivial elements of the acceleration R-matrix at location z are:

$$R_{13} = R_{24} = 2\Delta z\,/[1+(\eta_-)^{1/2}] \quad , \tag{4}$$

$$R_{22} = R_{44} = R_{66} = 1/(\eta_-)^{1/2} \quad , \tag{5}$$

and

$$R_{56} = \Delta z\,/\gamma^2 \quad , \tag{6}$$

where

$$\eta_- = V(z)/V(z-\Delta z) \quad , \tag{7}$$

and γ is the relativistic energy factor of the beam at z. The non-trivial elements of the lens R-matrix are:

$$R_{21} = R_{43} = -\,[\eta_-\eta_+ - 2\eta_- + 1]/(4\eta_-\Delta z) \quad , \tag{8}$$

where

$$\eta_+ = V(z+\Delta z)/V(z) \quad . \tag{9}$$

The space charge R-matrix is modeled following the general procedure utilized in TRACE 3-D. The technique is described in detail in Reference [1] and will not be discussed here. However, TRACE 3-D was developed to model bunched beams, rather than continuous (DC) beams of the type most commonly of interest for electrostatic systems. Consequently, the initial longitudinal phase space parameters and beam current input to TRACE 3-D need to be modified, so that the beam becomes essentially 2-D in character. Specifically, the effective bunched beam current in

TRACE 3-D, I, for a bunch with half-length r_z, is related to the continuous beam current, J, for an equivalent DC beam by:

$$I = (4/3)(r_z/\beta\lambda)\, J \quad , \tag{10}$$

where β is the relativistic velocity parameter (v/c) for the initial beam and λ is the wavelength of the radiofrequency defining the time interval between bunches. For a beam with a fractional momentum spread half-width of $\Delta p /p$, the longitudinal emittance ε_z is given by:

$$\varepsilon_z = r_z(\Delta p /p) \quad \pi\text{-meter-radian} \quad , \tag{11}$$

when r_z is given in meters. The corresponding longitudinal Twiss parameters are:

$$\alpha_z = 0 \quad , \tag{12}$$

$$\beta_z = r_z / (\Delta p /p) \quad \text{meter/radian} \quad , \tag{13}$$

and

$$\gamma_z = (\Delta p /p) / r_z \quad \text{radian/meter} \quad . \tag{14}$$

The procedure for setting up the modeling of a DC beam in TRACE 3-D is then straightforward. A scale length, L_s, is selected which is much larger than both (a) the physical length of the beamline under consideration and (b) the transverse size of the beam. The bunch half-length, r_z, of the beam is then set to equal L_s. For any given momentum spread ($\Delta p /p$) in the beam, then the longitudinal phase- space parameters are given by (11)-(13). The beam current is adjusted to that given by (10). (For the case where no radiofrequency components are in the beamline, the wavelength, λ, may also be set to equal L_s.) Using this procedure, the space charge fields of the TRACE 3-D bunch [1] are reduced to the space charge fields for a 2-D uniform beam [2]. The numerical accuracy of the procedure has been verified using TRACE 3-D by confirming that the radial expansion of cylindrical beams in the presence of high space charge reproduces the results of the semi-analytic solution for that case, which can be expressed in terms of Dawson's integral [7].

The formulas given by Equations (4)-(9) can be used to model any electrostatic element whose potential is given at discrete positions on the axis. Equations (10)-(13) provide a prescription for modeling DC beam space charge forces in TRACE 3-D. These results have been previously applied [5] to model a number of electrostatic einzel lenses, including the fringe fields. In this work, analytic forms for the on-axis potential functions are used for computing the R-matrix elements for the acceleration columns illustrated in Figure 1.

2.2 Potential Functions

The potential as a function of z for the electrostatic columns illustrated in Figure 1 may be written in terms of the electrode potentials V_1 and V_2 as:

$$V(z) = (V_1 + V_2)/2 + [(V_2 - V_1)/2]\ \phi(z) \quad , \tag{15}$$

where $\phi(z)$ is a monotonic function of z, and goes to ± 1 as z approaches $\pm\infty$. The function $\phi(z)$ depends only on the geometry (electrode spacings and dimensions) of the column.

For the two-aperture column illustrated in Figure 1(a), we use a potential that is a generalization of an equal aperture potential given by Szilagyi [8]. The generalization uses a superposition of the potentials for two thin apertures with unequal radii, R_1 and R_2, separated by a distance g. The result for the function $\phi(z)$ appearing in (15) is:

$$\phi(z) = (1/\pi)(g)^{-1}\{\mathrm{A}-\mathrm{B}\} \quad , \tag{16}$$

where

$$\mathrm{A} = (2z+g)\tan^{-1}[(z+g/2)/R_1] - 2R_1 \quad , \tag{17}$$

and

$$\mathrm{B} = (2z-g)\tan^{-1}[(z-g/2)/R_2] - 2R_2 \quad . \tag{18}$$

When $R_1 = R_2 = R$, this result for $\phi(z)$ reduces to that given by Szilagyi [8]. In the limit where $R_1 = R_2 = 0$, the function $\phi(z)$ reduces to a linear potential ramp from -1 to +1 over the distance g, and is equal to -1 for $z<g/2$, and +1 for $z>g/2$. To our knowledge, the potential model given by (16)-(18) has not been previously published

For the two-tube column shown in Figure 1(b), we use a potential given by Read, Adams and Soto-Montiel [5]. For that potential, the function $\phi(z)$ appearing in Equation (15) is:

$$\phi(z) = R\,(\omega' g)^{-1}\ln\{\mathrm{A}/\mathrm{B}\} \quad , \tag{19}$$

where

$$\mathrm{A}/\mathrm{B} = [(\omega z + \omega' g)/R\,] \;/\; [(\omega z - \omega' g)/R\,] \quad . \tag{20}$$

The constants ω=1.31835 and ω'=1.67. When $\omega'=\omega$=1.318, the potential is the same as one used by Lu, Ben-Zvi and Cramer [3] and other authors. The use of ω'=1.67 provides better agreement with numerical solutions to Laplace's equation for certain cases [5].

The fields are modeled to a distance d_1 before the column and to a distance d_2 after, so that the effective length of each column is $g + d_1 + d_2$. In the calculations described here, the values of $d_{1,2} = \mathrm{f}R_{1,2}$, where f is the TRACE 3-D fringe field extension factor, PQEXT [1].

3. COMPARISONS WITH OTHER WORK

Several calculations have been carried out using the electrostatic column models described above for comparison to other results available in the literature. Table 1 gives the focal length f obtained from TRACE 3-D for the 2-aperture lens when $R_1 = R_2 = R$, together with results from numerical calculations by Harting and Read [6], all expressed as the ratio $f_2/(2R)$. For $V_2/V_1 < 1$, the relation $f_2(V_2/V_1) = f_1/(V_1/V_2)$ has been used for the Harting and Read results. The computational uncertainty in the results of this work is approximately ±1 in the last significant figure given. This accuracy was obtained for $\Delta z/R = 0.01$. Three figure accuracy, adequate for most fitting and matching calculations, can be obtained using $\Delta z/R = 0.1$. For fringe fields extending ten radii before and after the column entrance and exit (f=10), the analytic model gives focal lengths typically within 3% (largest is 7%) of those given in [6] obtained from the numerical field solutions. Similar calculations have also been performed for the two-tube column, yielding similar comparisons to the Harting and Read [6] data for that type of column.

4. LOW ENERGY BEAMLINE APPLICATION

The two–tube and two–aperture electrostatic column models described above, together with the three–tube einzel lens models described previously [4], have been used in developing a model of the ion injection beamline and low energy acceleration sections of the HVEC Tandem Electrostatic Accelerator based system of the Center for Accelerator Mass Spectrometry (CAMS) at the Lawrence Livermore National Laboratory [9]. Figure 2 illustrates a PowerTrace [10] (TRACE 3–D) simulation of this ion beam transport system.

The two–tube columns (positions 8 and 17) have been used to simulate the insulating gaps that electrically isolate the magnet vacuum chamber from the upstream and downstream beamline components. In typical operation for $^{13}C^-$ and $^{14}C^-$, the potential of the vacuum chamber is switched in less than 100 μsec between 2 potentials (nominally –0.3 kV for 30 msec and –2 kV for 300 msec). These potentials are chosen so that the deceleration in the first gap and subsequent acceleration in the second gap allows the injected ion mass to be alternated between short pulses of the ^{13}C ions and longer pulses of the ^{14}C radioisotope.

The two–aperture columns (positions 24, 26 and 28) have been used to simulate the three important sections of the Dowlish Inclined–Field beam tubes of the HVEC FN Model Tandem accelerator at CAMS. The potentials across these tube sections are determined by the potential on the central terminal of the accelerator and the resistor values between the planes of the accelerator tubes within these sections. The first two–aperture–column in the model represents the initial half–voltage–gradient section of the first beam tube. The grid lens at the entrance of this section has been modeled by setting the entrance aperture radius to zero and inserting a thin lens model at the entrance; this combination both eliminates fringe field focusing at the entrance to the tube (which is one of the desired effects of the entrance grid) and allows the variable focusing provided by the entrance grid lenses to be modeled. The transition between the half–voltage–gradient and full–gradient sections, which occurs about 61 cm into the first tube section, has been modeled by setting both the exit radius of the first section and the entrance radius of the second section to zero and inserting a thin lens model between the two. The focal length of the thin lens has been set to the values expected for the injection of 39 keV $^{14}C^{-}$ ions and the voltage gradient transition for a central terminal voltage of 6.5 MV. The fringe field lens at the exit of the first beam tube has been modeled by setting the exit aperture radius at its physical value of 15 mm. The second beam tube has been modeled using a two–aperture–column with the physical entrance and exit radii of 15 mm and 8 mm, respectively.

The model of the ion injection beamline and low energy acceleration sections shown in Figure 2 has been set up using nominal normal operating values for the focusing elements and de/acceleration gaps and columns. The results obtained agree with experience gained in operating the beam transport system. The model indicates that, under normal operating conditions, the beam of interest is cleanly transported through the injection magnet, is well matched to the acceptance of the accelerator tubes, and produces a waist in the stripper canal that is approximately half the radius of the stripper canal. The clean transport of the ions of interest through our injection system and 100% transmission through our low energy acceleration sections is an essential requirement of our utilization of this system in accelerator mass spectrometry.

5. SUMMARY

Optical elements for electrostatic accelerator devices have been developed for use in the TRACE 3-D code. The elements, and a continuous (dc) beam space charge model, have been integrated into the TRACE 3-D version that works within the Shell for Particle Accelerator Related Codes (S.P.A.R.C.) software environment [10]. A detailed summary of the acceleration column models has been presented. Focal length calculations show good agreement with other results from the literature. The utility of the elements has been demonstrated in the development of a TRACE 3-D model of the low–energy injection line at the LLNL Center for Accelerator Mass Spectrometry.

ACKNOWLEDGEMENTS

Parts of this work were performed at LLNL under the auspices of the U.S. Department of Energy under contract W-7405-Eng-48. The work of Barrey W. Hill in developing improvements to the S.P.A.R.C. graphic user interface for TRACE 3-D is gratefully acknowledged.

REFERENCES

[1] K. Crandall and D. Rusthoi, "TRACE 3-D Documentation," third edition, Los Alamos National Laboratory Rep. LA-UR-97-886 (1997) 106 pages.

[2] D. C. Carey, *The Optics of Charged Particle Beams*, Harwood Academic Publishers (1987).

[3] J.-Q. Lu, I. Ben-Zvi and J. G. Cramer, "LYRAN: A Program for the Analysis of Linac Beam Dynamics" Nucl. Instru. Meth. Phys. Res. A 262 (1987) 200-6.

[4] G. H. Gillespie and T. A. Brown, "Optics Elements for Modeling Electrostatic Lenses and Accelerator Components I. Einzel Lenses," to be published in the proceedings of the 1997 Particle Accelerator Conference (1997) 3 pages.

[5] F. H. Read, A. Adams and J. R. Soto-Montiel, "Electrostatic Cylinder Lenses I: Two Element Lenses," J. Phys. E 4 (1971) 625-632.

[6] E. Harting and F. H. Read, *Electrostatic Lenses*, Elsevier Scientific Publishing Company, Amsterdam (1976).

[7] M. Reiser, *Theory and Design of Charged Particle Beams*, John Wiley and Sons, New York (1994), see p 199, Eqns. (4.38) - (4.40).

[8] M. Szilagyi, *Electron Ion Optics*, Plenum Press (1988), see p 84, Eqns. (3-183) and (3-184).

[9] J. R. Southon, M. W. Caffee, J. C. Davis, T. L. Moore, I. D. Proctor, B. Schumacher and J. S. Vogel, "The new LLNL AMS spectrometer," Nucl. Instr. Methods B52 (1990) 301-305.

[10] G. H. Gillespie and B. W. Hill, "A Graphical User Interface for TRACE 3-D Incorporating Some Expert System Type Features," 1992 Linear Accelerator Conference Proc., AECL-10728 (1992) 787-789.

Table 1. Focal length to aperture ratios, $f_2/(2R)$, for two 2-aperture acceleration columns, both with equal apertures ($R = R_1 = R_2$). Results of this work for two fringe field factors f are given, and compared to the calculations of Harting and Read [6].

	Acceleration Column with g/R = 1.0			Acceleration Column with g/R = 2.0		
V_2/V_1	$f_2/(2R)$=-1/(2R R_{21}) [this work] f=2.5	f=10.0	$f_2/(2R)$ [6]	$f_2/(2R)$=-1/(2R R_{21}) [this work] f=2.5	f=10.0	$f_2/(2R)$ [6]
0.5	13.64	13.28	13.41	16.67	16.35	15.95
1.0	∞	∞	-	∞	∞	-
1.2	240.2	234.4	236.34	296.1	290.1	282.87
2.0	19.20	18.78	18.96	23.55	23.12	22.55
10.0	3.113	3.120	3.20	3.668	3.667	3.59
40.0	2.226	2.423	2.54	2.539	2.703	2.68
90.0	2.142	2.600	2.79	2.428	2.821	2.83
200.0	2.145	3.097	-	2.439	3.281	-

FIGURE CAPTIONS

Figure 1. Electrode geometries for the two electrostatic acceleration column models. Different potential functions are used to describe (a) a two-aperture column and (b) a two-tube column.

Figure 2. PowerTrace output for the ion injection beamline and low energy acceleration sections of the accelerator mass spectrometry system. The einzel lenses at 3, 6, and 20 have been adjusted to transport the ion beam (60 μA $^{14}C^{-}$) cleanly through the injection magnet and then to limit the beam width to match the acceptance at the entrance to the acceleration tubes (position 23). The focal length of the thin lens model (which represents a grid lens at the entrance to the accelerator tubes) has been adjusted to produce a waist at the position of the 1.2 cm diameter gas stripper canal (position 30).

Figure 1

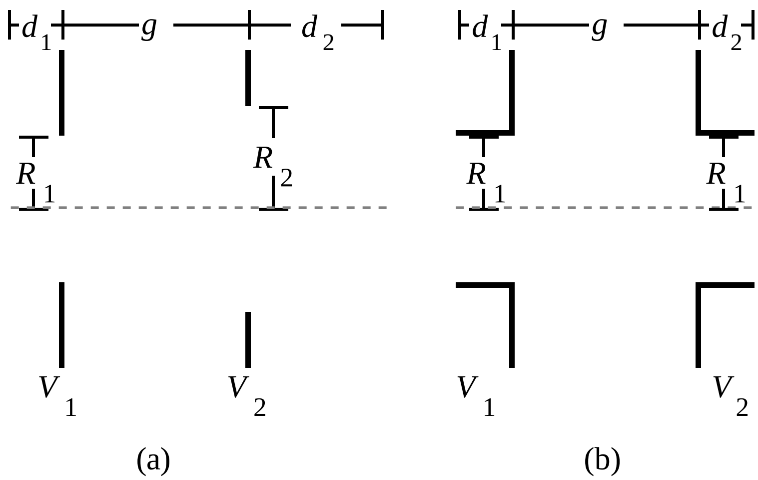

Figure 2

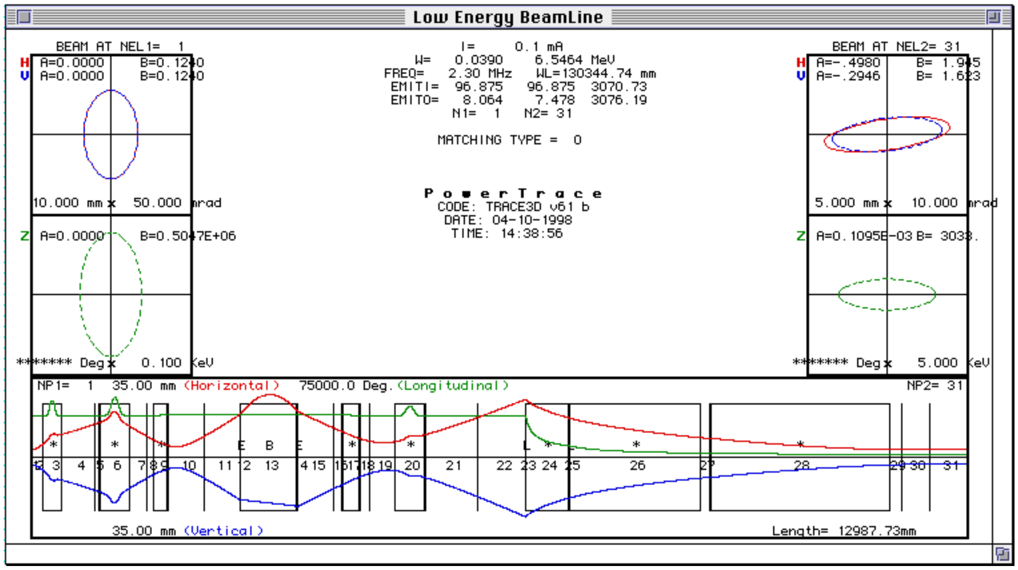
Low Energy BeamLine
BEAM AT NEL1= 1
A=0.0000 B=0.1240
A=0.0000 B=0.1240
10.000 mm 50.000 mrad
A=0.0000 B=0.5047E+06
******* Deg 0.100 KeV
I= 0.1 mA
W= 0.0390 6.5464 MeV
FREQ= 2.30 MHz WL=130344.74 mm
EMITI= 96.875 96.875 3070.73
EMITO= 8.064 7.478 3076.19
N1= 1 N2= 31
MATCHING TYPE = 0
PowerTrace
CODE: TRACE3D v61 b
DATE: 04-10-1998
TIME: 14:38:56
BEAM AT NEL2= 31
A=-.4980 B= 1.945
A=-.2946 B= 1.623
5.000 mm 10.000 mrad
A=0.1095E-03 B= 3033.
******* Deg 5.000 KeV
NP1= 1 35.00 mm (Horizontal) 75000.0 Deg. (Longitudinal)
NP2= 31
35.00 mm (Vertical)
Length= 12987.73mm

Technical Information Department • **Lawrence Livermore National Laboratory**
University of California • Livermore, California 94551